Experimental determination of the single-photon transition rate between the 2^3S_1 and 1^1S_0 states of He I†

Joseph R. Woodworth*‡ and H. Warren Moos
Department of Physics, The Johns Hopkins University, Baltimore, Maryland 21218
(Received 7 July 1975)

The highly forbidden single-photon transition rate between the 2^3S_1 and 1^1S_0 states of He I has been measured in a radio-frequency He discharge. The population of metastables in the 2^3S_1 state was determined by Fabry-Perot interferometric profiles of absorption from the 2^3S_1 to the $4^3P_{0,1,2}$ states. High spectral resolution and precision ultraviolet radiometry were used to determine the brightness of the emission feature observed at 625.54 ± 0.05 Å, compared to the theoretical value of 625.56 Å. Because of the very low transition rate, this feature is weak, but it is shown that it is due to the 2^3S_1-1^1S_0 transition. The value for the radiative transition rate obtained in these experiments was 1.10×10^{-4}/sec, with a 2σ uncertainty of $\pm 30\%$. A comparison to the theoretical value of 1.27×10^{-4}/sec is given. The relevance of this work to the beam-foil experiments which have measured the 2^3S_1-1^1S_0 transition rate for high-Z He-like ions is also discussed.

I. INTRODUCTION

In this paper a new measurement of the single-photon transition rate of the 2^3S_1-1^1S_0 transition in neutral helium is presented. The transition rate reported earlier[1] had an experimental uncertainty of a factor of 3. This report describes a new determination of the transition rate in which the experimental techniques were substantially improved. The details of the experiment are described in Sec. II, and the data obtained and their comparison with theory and other experiments are presented in Sec. III.

The transition rate of the 2^3S_1-1^1S_0 transition has been the subject of theoretical investigation since 1940, when Breit and Teller[2] considered the problem and concluded that the single-photon transition rate was only $\sim 10^{-24}$ sec^{-1}. They therefore concluded that the dominant decay mode of the 2^3S state would be a two-photon process with a transition rate of 1×10^{-5} sec^{-1}. This estimate of the two-photon transition rate was later reduced to 4×10^{-9} sec^{-1} by Drake, Victor, and Dalgarno.[3] In 1969, Gabriel and Jordan[4,5] identified a number of lines that had been observed in the solar x-ray spectrum as belonging to the *single*-photon 2^3S_1-1^1S_0 transition in heliumlike ions of oxygen, carbon, neon, sodium, and magnesium. Shortly thereafter, Griem[6] showed that the dominant decay mode of the 2^3S state in helium was a relativistically induced single-photon magnetic-dipole decay with a radiative transition rate of 0.5×10^{-4} sec^{-1}. More detailed calculations by Drake[7,8] and others[21] gave a transition rate of 1.27×10^{-4} sec^{-1}. These calculations also indicate that for He-like ions, in the limit of large Z the transition rate should scale as Z^{10}. Several authors have measured the 2^3S-state radiative lifetime for a number of high-Z He-like ions using heavy-ion accelerators and beam-foil techniques. Their results, with the stated uncertainties, are summarized in Table I and are compared with the theoretical values given by Drake.[7]

A measurement of the 2^3S-1^1S transition rate in He I tests the theoretical predictions at the opposite extreme from the beam-foil experiments, since the predicted radiative lifetime of the 2^3S state is more than ten orders of magnitude longer than the longest lifetime measured by beam-foil methods. If there were a competing radiative process with a transition rate varying differently from the Z^{10} dependence of the magnetic-dipole transition predicted by Drake, one would expect the discrepancy between experiment and theory to be very large by the time one reached helium, with $Z = 2$. In any case, the experimental determination of the radiative transition rate over a range of 10^{12} serves as an important check on the completeness of the theoretical analysis.

TABLE I. Radiative lifetimes of the 2^3S_1 state for high-Z ions.

Z	Element	Theoretical value (Ref. 7) (nsec)	Experimental value (nsec)	Reference (expt.)
16	sulfur	710	706 ±83	9
17	chlorine	381	354 ±24	9
17	chlorine	381	280 ±25	10
18	argon	212	172 ±12	11
22	titanium	27.4	25.8±1.3	11
23	vanadium	17.4	16.9±0.7	12
26	iron	5.0	4.8±0.6	12

II. EXPERIMENTAL TECHNIQUES

A. Apparatus

The theoretically predicted lifetime of 7870 sec precluded a direct observation of the time variation of a signal due to radiative decay as in the beam-foil experiments. Therefore, the procedure used here was to determine the brightness of the expected emission feature at 626 Å from a measured number of metastables to obtain the transition rate. The three basic requirements for this experiment were He discharge with a known number of $2\,^3S_1$ metastables in it, a high-resolution spectrometer of known throughput at 626 Å, and an absolutely calibrated detector for 626-Å photons.[13] A general description of the experimental setup is given in this section. In Sec. II B, the measurement of the quantum efficiency of the 626-Å photon detector is described. Section II C describes the measurement of the throughput of the spectrometer. In Sec. II D, the two methods of measuring the density of $2\,^3S_1$ metastables, both of which utilized absorption measurements from the $2\,^3S$ to the $4\,^3P$ state in the discharge, are discussed.

The limits given for the statistical errors in this experiment represent the 2σ limits (95% confidence level). For the uncertainties that are not statistical in nature, the quoted error bars are at least equal to the 95% confidence level.

A diagram of the apparatus used in this experiment is shown in Fig. 1. The discharge was excited in a 1.2-m-long, 12-cm-diam Pyrex tube with 0.045–0.68 Torr of high-purity (99.995% pure) He flowing through it. A differential pumping stage was used to keep He from entering the vacuum spectrometer. With this stage in place, the discharge tube could be operated up to 0.7 Torr without causing the pressure in the spectrometer to rise above 3×10^{-6} Torr. The discharge was excited by a 200-W commercial rf generator operating at 7 MHz. The spectrometer (McPherson Model 225) had a 998.9-mm radius-of-curvature concave replica grating overcoated with gold. The grating (2400 grooves/mm) produced a dispersion at the exit slit of 4.16 Å/mm. The entrance and exit slits were 27.7 μm wide for all of the $2\,^3S_1$-$1\,^1S_0$ measurements, which resulted in an observed instrumental linewidth of 0.115 Å at 626 Å. This resolution was necessary to resolve the 625.56-Å emission from continuum emissions due to the He_2 molecule.[14] In the previous experiment,[1] modulation of the discharge was used with time-resolved spectroscopy to suppress the continuum. In the present experiment, increases in spectral resolution, integration time, and metastable density permitted steady-state measurements, which significantly improved the quality of the data. In order to minimize the effects of astigmatism and small errors in the vertical alignment of the spectrometer, the entrance slit was made slightly taller (8.80 mm high) than the exit slit (8.06 mm high). The spectrometer was pumped through a Freon-refrigerated cold trap by a 6-in.-diam oil diffusion pump. Normal operating pressures in the spectrometer during these experiments were 3×10^{-6} Torr.

A channeltron with a sensitive area 9.0 mm in diameter (Bendix Model 4010) was used as the 626-Å photon detector. The dark count rate was 3 counts/min. The pulses from the detector were fed through a preamplifier and amplifier to a discriminator. The near-Gaussian pulse-height distribution of the detector permitted virtually all of the signal pulses to be counted without counting any of the low-level electronic noise in the system. This also greatly eased the requirements on the discriminator stability of the pulse-counting electronics necessary for accurate sensitivity calibrations. From the discriminator, the pulses were sent to a digital integrator (Fabritec 1062, denoted "analyzer" in Fig. 1) which stored and summed the data in the form of a histogram of counts vs time and hence wavelength. Data were collected in these experiments by repeatedly scanning the spectrometer (in a 2-min cycle) through a 5-Å region centered on 626.5 Å. During a cycle the spectrometer scanned down in wavelength for 1 min at a rate of 5.00 ± 0.02 Å/min, then reversed direction and scanned back to its starting point. Because of the extreme faintness of the 625.54-Å signal and the presence of a continuum background, it was necessary to accumulate the data from over 2000 scans of the spectrometer in the analyzer. The relatively bright (20000 counts/sec vs 6 counts/sec for the $2\,^3S$-$1\,^1S$ line) Ne I impurity line at 626.823 Å was used to assure that the spectrom-

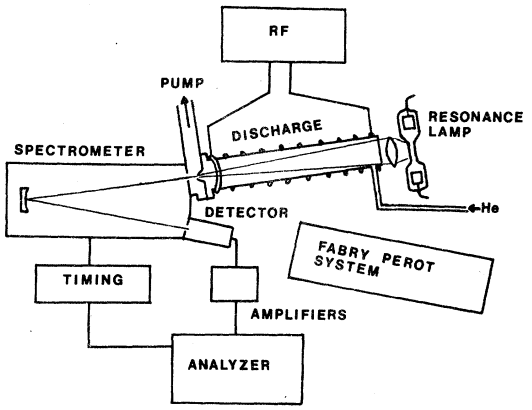

FIG. 1. Apparatus for measuring the $2\,^3S_1 \rightarrow 1\,^1S_0$ transition rate.

eter and the analyzer were synchronized. To start the analyzer scan, a second output from the pulse-counting circuits actuated a Schmidt trigger on the rise of the 626.823-Å line as the spectrometer scanned down towards 625.54 Å. This method, owing to the sharpness of the rise of the Ne I line, was not very sensitive to small drifts in the intensity of the discharge and was repeatable to ±0.016 Å.

A typical run lasted for several days. At least once every 24 h during the experiments, the density of metastables in the discharge was calibrated by a low-resolution absorption method described in Sec. IID. Between these calibrations, the intensity of the Ne I 626.8-Å line was monitored as a relative indicator of fluctuations in the discharge. (The 626.8-Å line was so close to the He 2^3S_1-1^1S_0 energy gap that it was strongly pumped by collisions with He 2^3S metastables.[15] Hence, it provided a sensitive indicator of fluctuations in the 2^3S metastable density.)

B. Detector efficiency calibrations

The efficiency of the detector was determined by comparing its response at 601 Å to the response of an Ar-filled (99.997% purity) double-ionization chamber based on the design of Samson.[16] Canfield *et al.*[17] have shown experimentally that Ar has a quantum efficiency of unity. The 601-Å photons from He_2^* emissions were provided by the large discharge tube and 1-m spectrometer described previously. A double-ionization chamber was used only to assure that all (>99%) of the photons were absorbed before reaching the rear wall of the chamber. To keep the ~0.3 Torr of Ar out of the spectrometer, a differential pumping stage was inserted between the ionization chamber and the spectrometer. To determine that the ionization chamber was operating properly, the current from the chamber versus voltage on the collector plates was measured (see Fig. 2). In the region in which the gain and quantum efficiency of the chamber are equal to 1, the current through the electrometers should not depend upon the voltage on the collector plate. In Fig. 2 the curve of current vs voltage is flat for more than 10 V on either side of the operating point. To compare the detector to the ionization chamber, the detector and the ionization chamber were interchanged five or more times in sequence at the slit of the differential-pumping apparatus, and the signal levels were recorded in each case. This test was performed both before and after the 2^3S_1-1^1S_0 experiments were run, with identical results.

There was inevitably a small amount of argon gas in the differential-pumping chamber when the ionization chamber was in use. This gas absorbed a certain fraction of the 601-Å light. When the channeltron was placed on the differential-pumping chamber, this gas was no longer present, and hence the channeltron saw a slightly higher flux than the ionization chamber. The size of this effect was calculated from the measured argon pressure and optical path length in the differential-pumping system and the total absorption cross section of argon for 601-Å photons. (The ionization chamber was used to measure the third quantity.) The gas in the differential-pumping system normally caused a correction of a factor of 1.17 to the quantum efficiency of the channeltron. The uncertainty in this correction due to the uncertainty in the gas pressure in the differential pumping chamber was ±50%. A correction of ~1.10, due to the dead time of the discriminator in the pulse-counting electronics, was also made. [Hence (quantum efficiency) = (raw data) × 1.10/1.17.]

The entrance slit in front of the ionization chamber and channeltron during these calibrations was 8 mm high and 0.7 mm wide, approximating the exit slit of the 1-m spectrometer. Thus, the area of the channeltron calibrated was the same as that used during the 2^3S_1-1^1S_0 transition experiments. Curves of quantum efficiency vs wavelength supplied by the manufacturer are flat, showing a change of less than 2% from 600 to 650 Å. Thus the adopted 10% uncertainty, arising from the fact that the channeltron was calibrated at 601 Å but used at 626 Å, is conservative. The value of the quantum efficiency at 626 Å obtained from these measurements was 0.145, with a 2σ uncertainty of ±13%.

C. Throughput of the spectrometer

The throughput of the spectrometer was determined by the area of the slits, the solid angle of

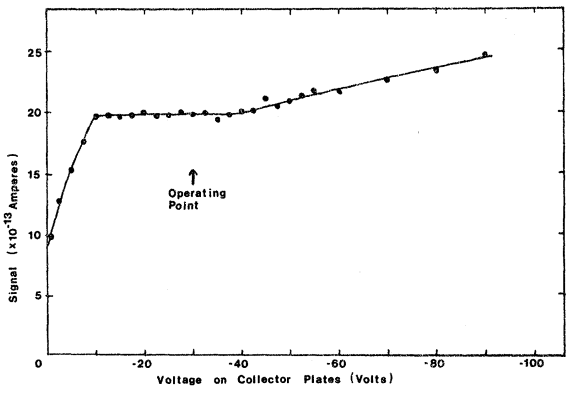

FIG. 2. Signal current from the Ar ionization chamber vs voltage on the collector plates. In the plateau region, the ion chamber operated as a detector with a quantum efficiency of unity.

the discharge illuminating the diffraction grating, and the reflectivity of the grating at 626 Å. The widths of the slits were set at 27.7 ± 1.3 μm. The height of the exit slit was 8.06 ± 0.02 mm. The ruled area of the diffraction grating was 15.0 ± 0.1 cm^2. However, owing to a very slight amount of vignetting of the grating by the differential-pumping mechanism, the effective area of the grating was reduced to 14.85 ± 0.15 cm.

To measure the reflectivity of the diffraction grating used in the $2\,^3S \rightarrow 1\,^1S$ rate experiment, a 50-cm premonochromator was used to provide a monochromatic input beam to the 1-m monochromator. To measure the reflectivity of the grating in the 1-m monochromator at a particular wavelength, both monochromators were set for that wavelength and the total flux entering and leaving the 1-m monochromator was determined. To make this measurement, the signals were measured from a channeltron mounted behind the exit slit of the 1-m monochromator and a second channeltron mounted behind its entrance slit. (The second channeltron was mounted on a slide so that it could be moved into and out of the light beam.) The relative efficiency of these two detectors was calibrated in a separate experiment. The light source for these measurements was a small rf-excited lamp with ~0.5 Torr of a 4-to-1 mixture of He and Ne flowing through it. The lamp was connected to the 50-cm premonochromator by a 1-mm-diam pinhole which also served as the entrance slit for the premonochromator.

The average reflectivity of a 2.54-cm^2 area in the center of the 1-m grating was measured using the He I line at 584 Å and the Ne I lines at 626 +629 and 735 +745 Å. To test for uniformity of reflectivity across the surface of the grating, the relectivity of six smaller areas (covering a total of ~80% of the ruled area) was measured at 584 Å. These measurements were made by placing a small aperture over the 50-cm grating and inserting a plate with a 1° wedge in various orientations between the two monochromators. These small-area measurements disclosed a 20% variation in reflectivity from one side of the grating to the other. However, as this variation was very nearly linear across the grating, it was necessary only to adjust the average reflectivity values upwards by 3% to obtain a value for the reflectivity representing the entire surface of the grating.

Light reflected from gratings may be partially polarized. Consequently, the reflectivity measured in a calibration such as the one above may depend on the relative orientation of the rulings of the two gratings. To check for this effect, rotating vacuum seals were built into the 50-cm spectrometer so that it could be rotated 90° about its optic axis. Thus the reflectivity of the 1-m grating was tested both when the rulings on the two diffraction gratings were parallel and perpendicular to each other. The difference between two measurements was less than 3% and was not considered significant.

The measured reflectivities of this diffraction grating corrected for the nonuniformities are listed in Table II. These values are consistent with the normal incidence reflectivity of gold,[16] and the fact that this grating was very strongly blazed in first order at 800 Å.

D. Metastable density measurements

The density of metastables was determined by measuring the fraction of the 3188-Å ($2\,^3S_1$-$4\,^3P_{0,1,2}$) radiation from a resonance lamp which was absorbed by the large discharge tube. As shown in Fig. 1, the radiation from the lamp was imaged through the discharge tube onto the spectrometer entrance slit. The light then passed through the spectrometer in zero order and the percent absorption was analyzed by one of two methods.

First, the metastable density was determined by measuring the total absorption[18] of the 3188-Å line with a photomultiplier tube behind an interference filter mounted at the exit slit. This was the most convenient method and was used in the 626-Å emission brightness experiments. However, this measurement could have had systematic errors, and therefore a high-resolution technique was used to check the low-resolution measurements.

In the second method, the absorption coefficient vs frequency for the 3188-Å absorption line was measured by replacing the photomultiplier and filter with a lens which relayed the 3188-Å light to a Fabry-Perot interferometer system. In this system, a lens imaged the center of the fringe pattern from the elaton onto a screen with a $\frac{1}{2}$-mm-diam pinhole. A broadband interference filter centered at 3200 Å and a photomultiplier tube were mounted directly behind the pinhole. The spectrum was scanned by varying the pressure of air between the two Fabry-Perot plates. This pressure-scanned Fabry-Perot system had a free spectral range of 0.126 Å and a resolution of 0.007 Å at 3188 Å.

Typical spectra of the 3188-Å lines from the

TABLE II. EUV grating reflectivity.

Wavelength (Å)	R	2σ uncertainty (%)
584	0.073	15
626 +629	0.073	16
735 +743	0.077	15

resonance lamp, discharge, and discharge plus resonance lamp are shown in Fig. 3, along with spectra from a ^{198}Hg lamp. The metastable densities were calculated from both the high- and low-resolution measurements by the standard methods described by Mitchell and Zemansky.[18] (The fine-structure splitting of the 3188-Å line was accounted for in these calculations.) The value of the absorption oscillator strength of $(2.577 \pm 0.002) \times 10^{-2}$ for the $2\,^3S$-$4\,^3P$ transition was taken from Schiff, Pekeris, and Accad.[19] For the calculations from the low-resolution measurements, the Doppler widths of the 3188-Å emission and absorption lines were obtained from the Fabry-Perot data. Metastable densities were measured only with the low-resolution technique during the $2\,^3S$-$1\,^1S$ transition experiments and the low-resolution measurements were cross calibrated against the Fabry-Perot measurements later. Cross calibrations were performed at each of the discharge-tube pressures of 0.045, 0.28, and 0.68 Torr.

After the low-resolution measurements were corrected for the fact that the 3188-Å line has two overlapping components, the densities calculated from the low-resolution measurements were still an average of 8% higher than the Fabry-Perot measurements. However, 8% corresponds roughly to the uncertainty in the 3188-Å emission and absorption linewidths used in the low-resolution calculations. Thus the Fabry-Perot measurements were assumed to be correct and the low-resolution values were adjusted downward by a factor of 1.08. Typical metastable densities for all of these experiments were 1.4×10^{11} cm^{-3}. The total uncertainty in these measurements was ±12%. Nonuniformities in the discharge were investigated and were found to have an effect on the measured value of the $2\,^3S_1$-$1\,^1S_0$ transition rate less than 1%.

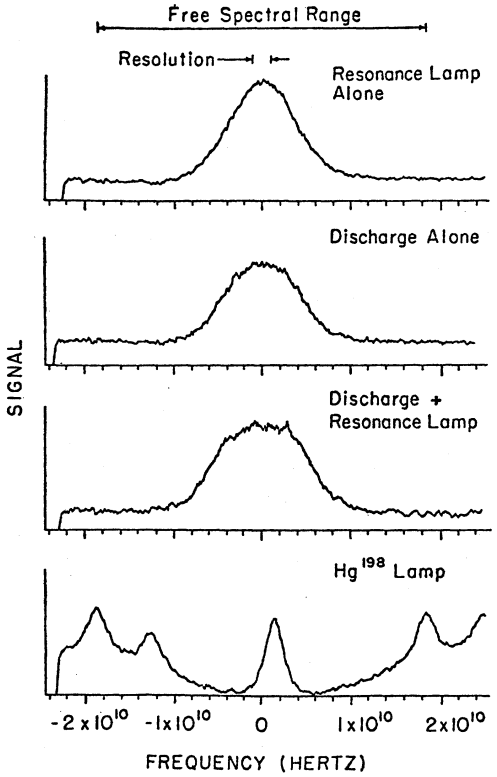

FIG. 3. Fabry-Perot fringes for 3188-Å emission lines from the resonance lamp, discharge, and discharge plus resonance lamp. The free spectral range and resolution of the instrument are indicated. The 3126-Å line from a ^{198}Hg lamp (centered) is shown for comparison. Two orders of the 3131-Å lines from this lamp are also visible.

III. RESULTS

A. Transition rates

The data from the $2\,^3S_1$-$1\,^1S_0$ transition experiments are shown in Fig. 4. The pressure in the

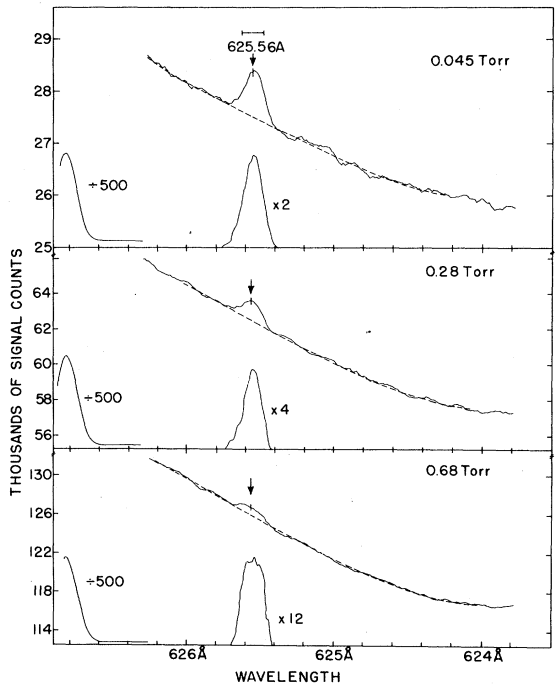

FIG. 4. Emission from the discharge at three different pressures. The strong line is due to Ne I. There is clearly a feature at 625.54 ± 0.05 Å superimposed on the sloping continuum. This figure is shown with the base line subtracted at the bottom of each graph. The signal counts were recorded in 0.0083-Å intervals. A sliding average of 10 was taken so that only every 0.083-Å interval contains completely independent data. Note that the ordinate scales for each pressure are different. The bar indicates spectral resolution.

discharge tube was varied to check for pressure-dependent effects. In each graph of Fig. 4 the relatively strong Ne I line at 626.823 Å is shown with its intensity divided by 500. The predicted location of the 626.56-Å emission feature due to the $2\,^3S_1$-$1\,^1S_0$ transition is marked by an arrow. In each run of the experiment, there is clearly a feature superimposed on the background at this wavelength. This feature, with the background subtracted, is shown at the bottom of each graph. The background level in each experiment was determined by a fourth-degree polynomial fit to the continuum on either side of the line.

The brightness B in counts per second of the 625.5-Å line as seen by the detector in this experiment is given by

$$B=(A/4\pi)NlA_sA_gRQ/F^2$$

where A is the radiative transition rate into 4π sr, Nl the number of $2\,^3S_1$ metastables in a 1-cm^2 column length of the discharge, A_s the area of the slits, A_g the area of the grating, R the reflectivity of the grating, Q the quantum efficiency of the detector, and F the focal length of spectrometer. The radiative transition rate is then obtained from the experimental data by

$$A=4\pi TF^2/NlEA_sA_gRQ\,, \qquad (1)$$

where T is the total number of counts in the 625.54-Å line and E is the "equivalent time." The equivalent time that the detector viewed the emission line is defined as the time the spectrometer spent passing through the full width at half-maximum of the ideal, slit-limited, triangular instrumental function of the spectrometer. Since only the total intensity of the emission line was used to determine the transition rates, it did not matter that the actual line shape was not perfectly triangular. For this system, the equivalent time the detector viewed the 625.54-Å feature accounted for only 1.38 sec out of each 120-sec scan of the spectrometer.

Using Eq. (1), the transition rates for each of the three sets of data shown in Fig. 4 were determined. Table III shows the total number of counts in the 625.54-Å emission line, the equivalent time the detector viewed the line, and the calculated transition rate for each of the three runs.

B. Evidence that the emission feature observed at 625.54 Å is due to the $2\,^3S$-$1\,^1S$ transition

In this experiment, a small signal was measured on top of a large background in the presence of nearby emission lines which were many orders of magnitude brighter. Therefore, it was necessary to determine whether the feature observed at 625.54 Å was really due to the $2\,^3S$-$1\,^1S$ transition or was due to an impurity line in the discharge, a grating ghost, or a feature in the continuum.

A number of tests which were run to test the linearity of the grating drive screw in the 1-m spectrometer failed to show any error as large as 2% in the relative location of any two spectral lines. 2% of the distance between the feature at 625.54 Å and the 626.823-Å Ne I line corresponds to 0.025 Å. Thus, the location of the emission feature observed in this experiment is conservatively stated to be 625.54 ± 0.05 Å, compared to a theoretical value of 625.56 Å. The extensive ultraviolet atomic and ionic emission-line list by Kelly[20] showed no atomic or ionic emission lines (either in first or second order of the spectrometer) closer than 0.30 Å to 625.56 Å, indicating that the observed feature was not an atomic or ionic impurity line.

In an earlier set of experiments,[1] the large discharge tube was pulsed at 1000 Hz and data were collected only in the afterglow of each pulse. In the afterglow, all of the atomic emission lines, except the 626.82- and 629.74-Å lines, were more than a factor of 50 weaker than when the discharge was on continuously. Using present values of grating reflectivity and detector efficiency, the transition rates obtained from the pulsed experiments range from 1.2–2.0×10^{-4} sec^{-1}, with an uncertainty of a factor of 3, in excellent agreement with the 1.10–1.12×10^{-4} reported in this paper. Thus the fact that the 625.54-Å feature was not a factor of 50 weaker during the pulsed experiments indicated that it was not a ghost of any of these emission lines. However, the 626.82- and 629.74-Å Ne I lines were not attenuated during the afterglow because, as mentioned previously, they were so close to the $2\,^3S$-$1\,^1S$ energy gap that they were very effectively pumped by collision with the He $2\,^3S$ metastables. It was still possible to rule out a ghost of these lines, though, by comparing the results at different pressures. The ratio of the 626.8-Å to 629.7-Å lines was roughly constant with pressure, but the absolute intensity of the 626.8-Å line varied by almost a

TABLE III. Experimental transition rates.

Pressure (Torr)	Total counts in line	Equivalent time (sec)	Transition rate (sec^{-1})
0.045	16983	3169	1.10 ± 10^{-4}
0.28	20164	3439	1.12 ± 10^{-4}
0.68	15452	3218	1.12 ± 10^{-4}

TABLE IV. Transition rates vs pressure with relative error bars.

Pressure (Torr)	Transition rate (sec)	1σ relative uncertainties (%)
0.045	1.10×10^{-4}	±7
0.28	1.12×10^{-4}	±8
0.68	1.12×10^{-4}	±17

TABLE V. Upper limits on collision-induced transition.

Pressure (Torr)	P (%)
0.045	2
0.28	12
0.68	28

factor of 10 with pressure during the earlier pulsed experiments[1] and by more than a factor of 4 during the present experiments. The fact that there was no comparable variation in the intensity of the 625.54-Å line indicated that it was not a ghost of one of these two lines.

The background continuum under the 625.54-Å line was composed primarily of He_2 molecular bands. Although no fine structure was observed in any of these bands, there was always the possibility that there was some feature in the continuum at 625.54 Å. However, the level of the continuum was a factor of 4.5 higher in the high-pressure runs than in the low-pressure runs. Therefore, any continuum feature large enough to cause an observable effect on the value obtained for the transition rate at low pressure should have caused a large change in the transition rate during the high-pressure experiments. The fact that no such effect was observed indicates that continuum features were not important, at least during the low-pressure experiments.

C. Examination of pressure-dependent effects

The spontaneous transition rate of the $2\,^3S$-$1\,^1S$ transition is a constant and cannot depend upon the pressure in a light source. Therefore, if the transition rate measured in this experiment varied with pressure, it would indicate that the quantity measured was not the spontaneous-emission rate, but some combination of this rate and a rate for collision-induced transitions, or a fluctuation in the background, as discussed previously. An upper limit on this type of effect may be determined from comparing the transition rates obtained when the discharge-tube pressure was varied. The measurements at the three different pressures and their 1σ error bars relative to each other are listed in Table IV.

It was assumed that the maximum difference in total transition rate permitted by the 1σ relative uncertainties could be expressed as

$$\delta W = K\delta P, \tag{2}$$

where δW is the maximum possible change in observed transition rate, δP the difference in pressure, and K the constant due to collision-induced transitions. From the data in Table IV and Eq. (2) upper limits were set on the percentage P of the total transition rate that could have been due to collision-induced transitions. These upper limits are shown in Table V. It should be stressed that the values given in Table V are only upper limits. The values for the $2\,^3S$-$1\,^1S$ transition rate obtained at the three different pressures differed from each other by less than 3%, and the much larger upper limits in Table V are due only to the relative uncertainties of the measurements at the

TABLE VI. Calibration uncertainties.

Source	Uncertainty (%)
Metastable density determinations	12
Grating reflectivity measurements at 626 Å	16
Detector efficiency at 626 Å	13
Widths of spectrometer slits	7
Vignetting of grating	1
Accuracy of spectrometer alignment	2
Fluctuations in metastable density during experiments	6

TABLE VII. Total uncertainties in transition rates.

Pressure (Torr)	Transition rate (sec^{-1})	Calibration uncertainties (%)	Statistical error (%)	Background subtraction (%)	Total uncertainty (%)
0.045	1.10×10^{-4}	±26	±13	±6	±30
0.28	1.12×10^{-4}	±26	±15	±3	±30
0.68	1.12×10^{-4}	±26	±25	±24	±43

three pressures.

The 625.54-Å line shapes obtained during the experiments at 0.045 and 0.28 Torr match the instrumental line shapes of the 1-m spectrometer to within a few percent, indicating that the width of this emission line is 0.04 Å or less. At 0.68 Torr, however, the 625.54-Å feature is noticeably broadened.[13] This broadening could be due either to a feature in the continuum which is beginning to become significant or to an incipient pressure-dependent effect in the $2\,^3S$-$1\,^1S$ transition rate. In any case, because the low-pressure data was used for the final value, any incipient high-pressure effects are not significant.

D. Error analysis, comparison with theory, and other measurements

To compare the values of the transition rate obtained in this experiment with theoretical values, the total uncertainties in the experimental values of the transition rate must be known. A summary of the 2σ uncertainties in each of the calibrations is given in Table VI. Since these are all independent sources of error, the total 2σ calibration uncertainty was ±26%. To obtain the total uncertainty in the transition rates, the statistical uncertainty in the data and the error in subtracting the base line had to be added to the calibration uncertainties. The 1σ statistical error in the data was taken as the square root of the total number of counts in the line and the base line underneath it. To determine the error in subtracting off the base line, the mean deviation of the data from the base line was determined for a number of linewidth-wide segments of the continuum on either side of the 625.54-Å line. The standard deviation of these means from zero was taken as the 1σ error in subtracting off the base line. The 2σ uncertainties due to these effects plus the calibration uncertainties are given in Table VII.

The theoretical transition rate for the $2\,^3S$-$1\,^1S$ transition given by Drake[7] of 1.27×10^{-4} sec^{-1} is within the 2σ limits of all of the data taken in this experiment. Taking the value obtained at 0.045 Torr as both the most accurate value and the one which is least likely to have been influenced by pressure-induced transitions, the spontaneous transition rate of the $2\,^3S_1$-$1\,^1S_0$ transition observed in this experiment was 1.10×10^{-4} sec^{-1}, with a 2σ uncertainty of ±30%.

Early beam-foil measurements of $2\,^3S_1$ radiative lifetimes in high-Z He-like ions showed a tendency toward shorter lifetimes than the theoretical calculations for the lower-Z ions. This discrepancy has been shown to be due to experimental details, and is not real. The transition rate for the $2\,^3S_1 \rightarrow 1\,^1S_0$ transition is more than a factor of 10^{10} smaller than the smallest rate measured by beam-foil techniques. If there were an unaccounted-for effect on the transition rate, it should vary smoothly with Z; for instance, as Z^N where $N \neq 10$; this would cause a very obvious discrepancy between theory and experiment for He. In fact, no evidence of any such discrepancy was observed (see Fig. 5). Thus by fixing the value of the transition rate at low Z this experiment highly determines the possible values over the range of Z and thus theoretical values at intermediate values of Z may be used with confidence.

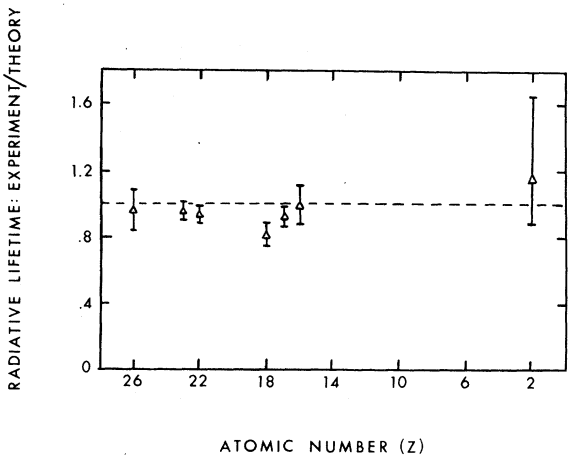

FIG. 5. Comparison of experimental and theoretical $2\,^3S_1$ lifetimes for various values of Z.

†Work supported in part by the National Aeronautics and Space Administration under Grant No. NGR-21-001-001.

*Present address: Sandia Laboratories, Org. 5216, Albuquerque, N.M. 87115.

‡National Science Foundation Trainee.

[1]H. W. Moos and J. R. Woodworth, Phys. Rev. Lett. 30, 775 (1973).

[2]G. Breit and E. Teller, Astrophys. J. 91, 215 (1940).

[3]W. F. Drake, G. A. Victor, and A. Dalgarno, Phys. Rev. 180, 25 (1969).

[4]A. Gabriel and C. Jordan, Nature 221, 947 (1969).

[5]A. Gabriel and C. Jordan, Mon. Not. R. Astron. Soc. 145, 241 (1969).

[6]H. R. Griem, Astrophys. J. 156, L103 (1969).

[7]G. W. F. Drake, Phys. Rev. A 3, 3 (1971).

[8]G. W. F. Drake, Phys. Rev. A 5, 5 (1972).

[9]J. A. Bednar, C. L. Cocke, B. Curnutte, and R. Randall, Phys. Rev. A 11, 460 (1975).

[10]C. L. Cocke, B. Curnutte, J. MacDonald, and R. Randall, Phys. Rev. A 9, 57 (1974).

[11]H. Gould, R. Marrus, and R. W. Schmeider, Phys. Rev. Lett. 31, 504 (1973).

[12]H. Gould, R. Marrus, and P. J. Mohr, Phys. Rev. Lett. 33, 676 (1974).

[13]For a more detailed description of the experiment, see the Ph.D. thesis by J. R. Woodworth (Johns Hopkins University, 1974) (available through University Microfilms, Ann Arbor, Michigan).

[14]Y. Tanaka and K. Yoshino, J. Chem. Phys. 50, 3087 (1969).

[15]A. Javan, W. B. Bennett, Jr., and D. R. Herriot, Phys. Rev. Lett. 6, 106 (1961).

[16]James A. R. Samson, *Techniques of Vacuum Ultraviolet Spectroscopy* (Wiley, New York, 1967).

[17]L. R. Canfield, R. G. Johnson, K. Codling, and R. P. Madden, Appl. Opt. 6, 1886 (1967).

[18]A. C. G. Mitchell and M. W. Zemansky, *Resonance Radiation and Excited Atoms* (Cambridge U. P., New York, 1934).

[19]B. Schiff, C. L. Pekeris, and Y. Accad, Phys. Rev. A 4, 885 (1971).

[20]R. L. Kelly, NRL Report No. 7599 (1973).

[21]G. Feinburg and J. Sucher, Phys. Rev. Lett. 26, 681 (1971).